In: Encyclopedia of Mathematics Research (3 Volume Set) ISBN: 978-1-61324-228-5
Editors: Joshua D. Mathias and Sophia I. Cleaves

Chapter 30

ELEMENTS OF NOZZLE DESIGN OPTIMIZATION

Vladislav M. Galkin[a]
Institute of Geology and the Oil and Gas Industries, Tomsk Polytechnic University,
30 Lenin Ave., Tomsk, 634050, Russia
Yuri S. Volkov[b]
Sobolev Institute of Mathematics, Siberian Branch of the Russian Academy of Sciences,
4 Koptyug Ave., Novosibirsk, 630090, Russia

ABSTRACT

In the framework of the ideal gas model, variational gas dynamics problems on optimum nozzle design are solved using a direct method. The model problems are two classical axisymmetric problems: the design of a supersonic nozzle with a corner point in the minimum cross section and a uniform exit characteristic and the design of a subsonic nozzle part with a plane sonic line in the minimum cross section. It is supposed that in both problems, the optimum nozzle profile must be a monotonic function. A priory information on the monotonicity of the desired profile is shown to be the one that allows a considerable increase in solution efficiency. A functional with a minimum corresponding to the optimum nozzle profile is selected taking into account the required monotonicity. For comparison, the desired nozzle profiles are described by polynomials and quadratic, cubic and rational splines. The varied variables are either profile expansion coefficients in terms of basis functions or the parameters to be interpolated. It is demonstrated that the problem solving is more efficient where the nozzle profile is represented as a monotonic function at each step of minimization. It is found that consideration of the peculiarities of the nozzle profile does much to determine the changeable part of a wind tunnel. In this problem, more efficient profile descriptions are those based on logarithmic functions and cubic splines with irregular nodes.

[a] E-mail address: vlg@tpu.ru
[b] E-mail address: volkov@math.nsc.ru

INTRODUCTION

Modern technologies necessitate the design of more and more advanced devices, and this is impossible without resort to numerical techniques. In this section, an attempt is made to generalize the experience of the authors in the field of optimum nozzle profiling based on a direct method.

The most versatile method of solving gas dynamics problems on a search for optimum aerodynamic shapes is the method of Lagrange multipliers [1]. However, this method allows an explicit solution for a rather narrow range of problems [2]; the resulting dependence of the optimum solution on the system of necessary extremum condition is most often implicit that considerably complicates the algorithms used. Therefore, simplified models, including Newton's law of resistance and local models [3], as well as, direct methods have received wide acceptance.

Direct computation consists in reducing a variational gas dynamics problem to nonlinear programming in which the desired contour is approximated by a function from a certain finite-dimensional and everywhere dense subspace and is uniquely described by the expansion coefficients $c_1,\ldots, c_N$ in terms of a given subspace basis [4]. There are two main procedures in the direct method: searching for an extremum function of N variables to minimize a certain functional (which minimum is the solution) and direct computation of the gas flow parameters inside a certain nozzle contour. The direct computation should be completed by computing the functional as a function of $c_1,\ldots, c_N$ with the minimization parameters as expansion coefficients $c_1,\ldots, c_N$ in terms of the basis [1]. The extremum is found by Broyden's quasi-Newton method with a quadratic convergence rate [5].

Practice shows that the main factor responsible for rather limited applicability of the direct method is the long CPU time due to repeated direct runs. Another factor affecting the method performance is that the contour in problem solving can be far from optimum. Figure 1 depicts contours obtained for a supersonic nozzle with a uniform exist flow. Apparently, the flow in contour *1* is mixed rather than supersonic, and this increases the computation time for the flow field. From the above considerations and our experience in the field, the emphasis is on the factors affecting the problem-solving speed in the direct method and, primarily, on the peculiarities of a problem responsible for:

(1) mathematical model;
(2) model problems;
(3) numerical technique used in direct computation with regard to the mathematical model;
(4) functional with a minimum corresponding to the optimum nozzle profile;
(5) method of nozzle description.

In this context, a model problem (sometimes, referred to as a test problem) is considered to mean a rather simple problem with a known or easily checked solution, which is convenient to use in numerical calculations for testing proposed ideas and verifying software implementation.

Note that most recent publications concerning numerical techniques refer to some extent or another to high-performance computing (HPC) and parallel computations. Despite the

undeniable urgency of HPC, we did not dwell on this method and algorithms in this chapter and all computations are made with a personal computer.

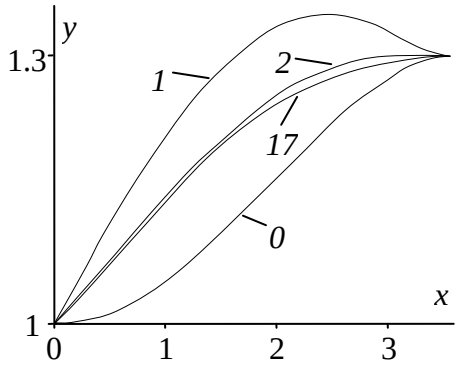

Figure 1. Supersonic nozzle with a uniform exit characteristic in a basis of 10 power polynomials: *0* – initial smooth profile; *17* – resulting profile with a corner point; *0*, *2*, and *17* correspond to the iteration index in the functional minimization.

1. MATHEMATICAL MODEL

Consider the gas flow in an axisymmetric nozzle which profile is given by the function $f(x)$. The gas is ideal (inviscid and non-heat-conducting), the flow is steady and is described by the equations:

$$\begin{aligned}
&\frac{\partial(y\rho u)}{\partial x}+\frac{\partial(y\rho v)}{\partial y}=0,\\
&\frac{\partial\left[y(\rho u^2+P)\right]}{\partial x}+\frac{\partial(y\rho uv)}{\partial y}=0,\\
&\frac{\partial(y\rho uv)}{\partial x}+\frac{\partial\left[y(\rho v^2+P)\right]}{\partial y}=P,\\
&\frac{\partial(y\rho uH)}{\partial x}+\frac{\partial(y\rho vH)}{\partial y}=0,
\end{aligned} \qquad (1)$$

where x and y – longitudinal and transverse coordinates; u and v – projections of the velocity vector on x and y axes; ρ and P – density and pressure; $H=P\gamma/(\rho(\gamma-1))+w^2/2$ – total enthalpy; $w^2=u^2+v^2$, γ – adiabatic index of the gas. Introduce the notations $M=w/a$; $a^2=\gamma P/\rho$; $S=P/\rho^\gamma$; $\tan\theta=v/u$; $\alpha=\arcsin(1/M)$; where M – Mach number; a – sound velocity; S – entropy function; θ – angle (or slope) of velocity vector to x axis; and α – Mach angle. Specified on the wall is the impermeability condition $\tan\theta=f'(x)$, where the

prime denotes the derivative with respect to x. The inlet boundary conditions are chosen depending on the type of equations (1) and are described below. At the nozzle exit, $M > 1$ in both problems, and hence boundary conditions are unnecessary. The dimensionless quantities are obtained though dividing x and y by the nozzle half-width in the minimum cross section; u and v, by the critical velocity a_*; ρ, by the critical density ρ_*; P, by the product $\rho_* a_*^2$, and H by the squared critical velocity a_*^2. It is assumed that the gas flows from left to right and $x = 0$ in the minimum cross section. Part of the computations was performed for an isoenergetic and isentropic (potential) flow:

$$\begin{aligned} H &= \text{const}, \\ S &= \text{const}, \end{aligned} \qquad (2)$$

and some of them for a complete system (1).

Further, we proceed from relations (1) and (2) to the characteristics equations and corresponding consistency conditions to be used below:

$$\frac{dy}{dx} = \tan(\theta \pm \alpha), \qquad (3)$$

$$d\theta \pm \frac{\cos^2 \alpha}{(\gamma+1)/2 - \cos^2 \alpha} d\alpha \pm \frac{\sin\alpha \sin\theta}{y \cos(\theta \pm \alpha)} dx = 0. \qquad (4)$$

Equations (3) and (4) specify two families of lines: C^+ and C^- depending on the plus or minus sign, respectively. The characteristic C^0 fits the equation:

$$\frac{dy}{dx} = \tan\theta.$$

In addition to (1) – (4), it is convenient to use some of the exact solutions suitable for computations; namely, the Prandtl–Meyer formula relating the flow parameters in the rarefaction wave at the corner point:

$$\theta_2 + \omega(\alpha_2) = \theta_1 + \omega(\alpha_1) \qquad (5)$$

with

$$\omega(\alpha) = -\alpha + \sqrt{\frac{\gamma+1}{\gamma-1}} \arctan\left(\sqrt{\frac{\gamma+1}{\gamma-1}} \tan(\alpha) \right),$$

where indices 1 and 2 correspond to the parameters upstream and downstream of the corner point, and the equations for a uniform flow crosswise the nozzle passage:

$$\left(\frac{y_1}{y_2}\right)^2 = \frac{M_2}{M_1}\left(\frac{2+(\gamma-1)M_1^{\,2}}{2+(\gamma-1)M_2^{\,2}}\right)^{\frac{\gamma+1}{2(\gamma-1)}}, \quad (6)$$

where y is the passage width, M is the Mach number, and indices 1 and 2 correspond to the parameters at $x=x_1$ and $x=x_2$.

The choice of mathematical model (1) is explained as follows:

(1) only stationary processes are considered;
(2) most of the problems arising in numerical optimization can easily be solved by ideal gas equations;
(3) results obtained by ideal gas equations can serve as an initial approximation for more complex models;
(4) software implementation of the model in direct computation makes it possible to use fast algorithms, e.g. the explicit McCormack marching scheme or the method of characteristics in the supersonic region and a version of the factorization method in the transonic region.

An argument for the chosen model is the problem in a multimode hypersonic wind tunnel with a uniform flow in the operating region [6], in which, the supersonic contour was optimized using Navier–Stokes equations. The computations show that convergence of the optimization is possible only with a good initial approximation. This approximation was taken to be the resulting optimization with equations (1). The optimization time for the viscous statement was more than a day, and for the ideal gas – less than an hour.

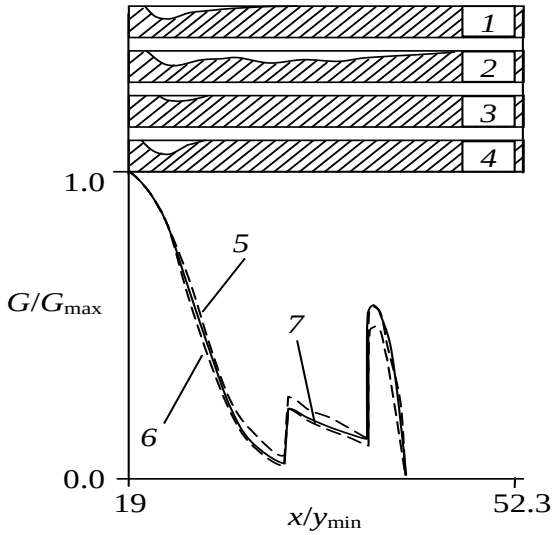

Figure 2. MHD part. Profilograms of the wall erosion from [10]: *1*, *2* – insulating walls; *3* – cathode, *4* – anode. *G* – calculated mass flows of the c-phase to the walls: *5* and *6* – cathode and anode at a maximum generated power; *7* – cathode, anode, and insulating walls in expulsion operations modes. $x = 0$ corresponds to y_{min}.

Another example is the problem on the design of the supersonic part of a nozzle with given dimensions for a pulse MHD generator [7]. In a plasma generator, Al-based solid fuel is employed; hence, the gas flow in the acceleration and conversion sections of the MHD generator involves precipitation of Al_2O_3 particles on the walls, resulting in the failure of the facility [8]. The computations show that we can ignore the electromagnetic terms, because of their moderate effect on the precipitation of the second phase, and replace three-dimensional by two-dimensional equations with parameters averaged over one coordinate [9]. In the inviscid model (viscosity is taken into account only in phase interaction coefficients), this makes possible a qualitative agreement with experiment (Figure 2 and [10]) and, using the Chebyshev polynomial approximation [11], a nozzle contour design with a less precipitated second phase.

Direct computation was used to solve the axisymmetric problem [12] on designing optimum supersonic nozzle parts for two-phase flows. As in the previous case, the gas was ideal and the viscosity was taken into account only in phase interaction coefficients.

The foregoing examples demonstrate that the inviscid problem is still urgent, though for a certain range of problems.

2. MODEL PROBLEMS

The model problems are two classical gas dynamics problems: the design of a diffuser transforming the uniform sonic (supersonic) flow at the inlet to a uniform flow at the exit [13], hereinafter, referred to as problem *a*, and the design of a confuser producing a plane sonic line in the minimum cross section [14], hereinafter, referred to as problem *b*.

These problems are examples of model problems, as well as, problems of practical interest. Problem *b* allows independent consideration of the subsonic and supersonic nozzle parts, and problem *a* is useful for designing maximum-thrust nozzles and supersonic wind tunnels with a uniform flow in the operating region, and shock-free air intakes [13].

The choice of the model problems is governed, primarily, by simple evaluation of the results obtained. For problem *a*, the solution per run is known and is found by the method of characteristics using the algorithm described in [15]. The algorithm consists in deviating from the plane sonic line, calculating the characteristics in the rarefaction wave until the specified Mach number M_0 is reached on the axis, and solving the Goursat problem between the calculated and uniform characteristics. In what follows, the nozzle contour computed with this algorithm is designated as a reference contour. Denote the multitude of contours with a plane sonic line at the inlet and a uniform flow at the exit (Figure 3) in terms of $W(\gamma,M_0,G)$. Here, through M_0 and G, we denote the exit Mach number and the ratio of the flow rate through the streamline used to design a nozzle to the flow rate of a nozzle with a corner point (for which, G=1).

Unfortunately, a simple solution to problem *b* is unknown; however, the final result is controlled from the shape and position of the sonic line. Hence, both problems are easily checked and are applicable as model problems. Note that the work of the authors Butov, Vasenin, Shelukha [4] is one of the pioneering publications in which the above model problems were used in numerical calculation.

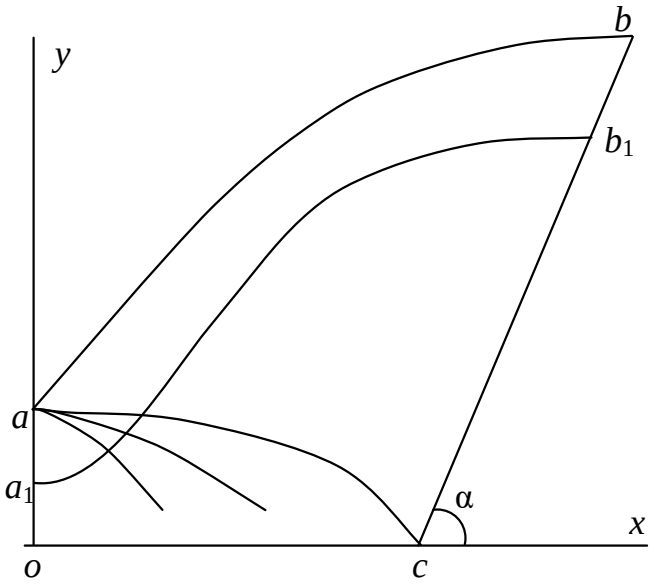

Figure 3. Family of nozzles $W(\gamma,M_0,G)$: *oa* – sonic line, *ab* – nozzle with a corner point and a flow rate $G = 1$, a_1b_1 – intermediate streamline for $G < 1$ (smooth nozzle), *ac* – characteristic C^-, *cb* – uniform characteristic C^+ with $\theta = 0$ and M_0, $\alpha = \arcsin(1/M_0)$.

Formulation of problem *a*. The coordinates x_b and y_b of the nozzle endpoint are given. The task is to find the contour of an axisymmetric supersonic nozzle $f(x)$ which satisfies the conditions:

$$\begin{aligned} &f(x_a) = y_a, \quad f(x_b) = y_b, \quad f'(x_b) = y_b', \\ &x_a = 0, \quad y_a = 1, \quad y_b' = 0, \end{aligned} \tag{7}$$

has $\theta_{in}=0$ and $M_{in}=1$, where the index *in* corresponds the nozzle inlet, and provides a uniform exit characteristic *cb* (Figure 4) with a zero slope and a constant Mach number equals to M_0:

$$\theta(\xi) = 0, \quad M(\xi) = M_0, \quad \forall \xi \in [cb]. \tag{8}$$

Note that formulation (7) and (8) admits both smooth nozzles and nozzles with a corner point in the section x_a, and, hence, $f'(x_a)$ is not given. Apparently, x_b and y_b cannot be given arbitrarily. The ordinate y_b and the exit Mach number M_0 are related by (6). For the abscissa x_b, there are three possible cases:

(1) Let x_b be equal to the length of a reference nozzle with a corner point and a uniform exit characteristic found, according to [15], from the given M_0. This nozzle is unique, since so is the solution of the Goursat problem.
(2) For x_b smaller than the length of a nozzle with corner point, a nozzle with a uniform exit characteristic (8) is impossible to design.

(3) And for x_b greater than this length, there exist infinitely many nozzles, namely, smooth nozzles constructed from intermediate streamlines and those with a corner point and a cylindrical extension. All these nozzles satisfy condition (8).

Therefore, the direct computation results were tested with the use of x_b corresponding to the unique solution, i.e. to the corner-point nozzle.

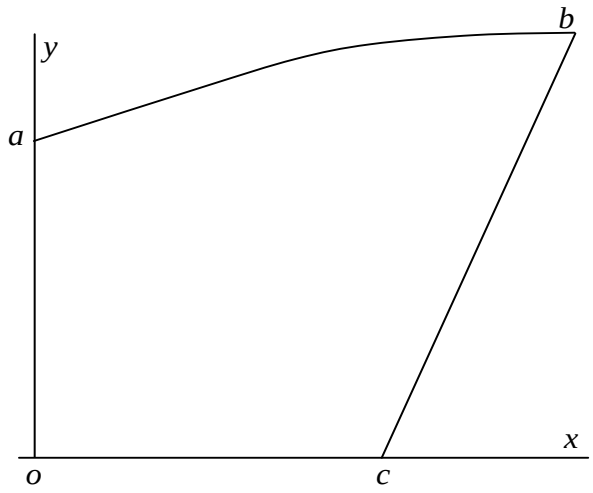

Figure 4. Model problem *a*: *oa* – minimum cross section, *ab* – desired nozzle with a corner point, *cb* – uniform characteristic C^+.

Formulation of problem *b*. Let a smooth profile $F(x)$ of the subsonic and small supersonic parts of an axisymmetric nozzle be described by:

$$F(x)=\begin{cases} y_a, & -2.5 < x < x_a, \\ f(x), & x_a \le x \le 0, \\ f_1(x), & x > 0. \end{cases} \qquad (9)$$

where $f_1(x) = 0.25(x+2)^3 - 0.75(x+2)^2 + 2$.

We are to find that part of the nozzle contour $f(x)$ (Figure 5) which satisfies the conditions:

$$\begin{aligned} &f(x_a) = y_a, \quad f'(x_a) = y'_a, \quad f(x_b) = y_b, \quad f'(x_b) = y'_b, \\ &x_a = -2, \quad y_a = 2, \quad y'_a = 0, \quad x_b = 0, \quad y_b = 1, \quad y'_b = 0 \end{aligned} \qquad (10)$$

and provides the position of the plane sonic line in the minimum cross section [4]. The expanding part in (9) at $x>0$ is required to obtain a supersonic flow at the right boundary of the computation domain and, hence, to eliminate the boundary conditions.

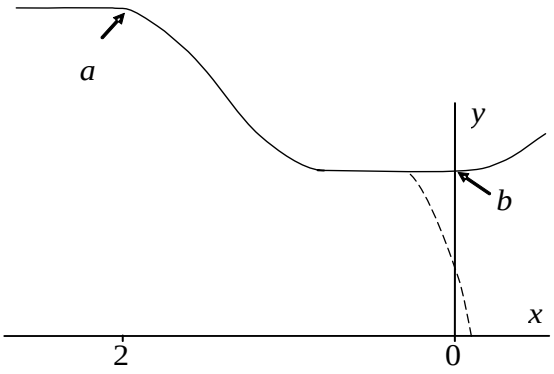

Figure 5. Model problem *b*: *ab* – desired nozzle part, dashed line – line M=1.

3. NUMERICAL METHODS

The choice of a numerical method for direct computation depends on two interrelated problems:

(1) unreasonable time of problem solving, which is associated with the ultimate computer speed;
(2) nonsimply connected functional domain and/or a solution inadequate to the physics of the process.

Consider problem *a*. Let the flow field in a certain nozzle with a profile determined by the varied variables $c_1,\ldots, c_N$ be calculated. The computed field is used to calculate the functional, characterizing the flow nonuniformity at the nozzle exit and featuring the minimum value for a uniform flow. The numerical realization of direct computation can be based on two approaches.

In the first approach, system (1) is hyperbolic, i.e. there exists only a supersonic flow, and simple and fast marching schemes, can be used.

In the second approach, the system of equations (1) is mixed, i.e. both supersonic and subsonic flows are possible, and hence, more complex and slower numerical techniques are required.

Let the first numerical implementation be based on the method of characteristics. Apparently, if in a certain nozzle, the flow is subsonic or the characteristics of one family intersect, an abnormal end (abend) of computation occurs. Thus, the domain of the functional is nonsimply connected, since the functional that uses the flow parameters at the nozzle exit is impossible to calculate. The second approach, which takes into account the subsonic flow, normally employs relaxation techniques, of which the most reliable one is Godunov scheme capable of computing virtually all configurations with no abend. Unfortunately, relaxation is ineffective in terms of CPU time. In comparing the method of characteristics and Godunov scheme involving relaxation, it gives a ratio of 1:38 at the same computation accuracy, and in comparing the substitution of the explicit McCormack marching scheme [16] and Godunov

scheme involving relaxation, it gives a ratio of 1:91. Clearly, direct computation with Godunov scheme will be time consuming.

For this reason, problem *a* is solved by the method of characteristics (a nozzle with a corner point and a smooth nozzle of small length ≈ 4 [17]) or the McCormack marching scheme (a smooth nozzle of large extension ≈ 3000 [6]) with the method of functional evaluation changing in the case of abend situations (discussed below).

The use of two computational schemes in one problem is explained by the fact that for short nozzles with a corner point, the method of characteristics ensures a quite acceptable computation time, whereas, the McCormack scheme to involves the method of characteristics to correctly account for the corner point, and the algorithm is, thus, unreasonably complicated. For long nozzles, characteristic of hypersonic wind tunnels, the corner point is absent and this allows complete realization of the speed advantages of the simple scheme.

The McCormack scheme [16] is a two-step scheme of the predictor – corrector type:

$$\begin{aligned} \widetilde{A}_{i+1,j} &= A_{i,j} - \Delta x\left(\frac{B_{i,j+1} - B_{i,j}}{\Delta y} + C_{i,j}\right), \\ A_{i+1,j} &= \frac{1}{2}\left\{\widetilde{A}_{i+1,j} + A_{i,j} - \Delta x\left(\frac{\widetilde{B}_{i+1,j} - \widetilde{B}_{i+1,j-1}}{\Delta y} + \widetilde{C}_{i+1,j}\right)\right\}. \end{aligned} \tag{11}$$

A step is found from the relation: $\Delta x \le \sigma \Delta y \Big/ \max\left(\frac{|uv| + a\sqrt{u^2 + v^2 - a^2}}{u^2 - a^2}\right)$, where the coefficient $\sigma<1$ provides stability margin; *A*, *B*, and *C* correspond to the system of equations (1) in vector notation:

$$\frac{\partial A}{\partial x} + \frac{\partial B}{\partial y} + C = 0.$$

For the system of equations (3) and (4), the method of characteristics is realized using the modified Euler method as shown in Figure 6. Where *1–3* is a segment of C^+, *2–3* is a segment of C^-, and *3* denotes the point of their intersection. On the characteristics C^+ and C^-, *1* and *2* denote points with known parameters.

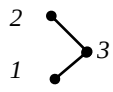

Figure 6. Design diagram of the method of characteristics.

Writing differential equations (3) in the difference form and denoting the iteration number j=1,2… yields the nonlinear system of equations to solve for the known parameters α_3^j, θ_3^j, x_3^j, y_3^j at point *3*:

$$
\begin{aligned}
&y_3^j - y_2 = (x_3^j - x_2)\tan(\theta_{23} - \alpha_{23}),\\
&y_3^j - y_1 = (x_3^j - x_1)\tan(\theta_{13} + \alpha_{13}),\\
&\theta_1 - \theta_3^j = \frac{\cos^2\alpha_{13}(\alpha_3^j - \alpha_1)}{(\gamma+1)/2 - \cos^2\alpha_{13}} + \frac{\sin\alpha_{13}\sin\theta_{13}(x_3^j - x_1)}{y_{13}\cos(\theta_{13} + \alpha_{13})},\\
&\theta_3^j - \theta_2 = \frac{\cos^2\alpha_{23}(\alpha_3^j - \alpha_2)}{(\gamma+1)/2 - \cos^2\alpha_{23}} + \frac{\sin\alpha_{23}\sin\theta_{23}(x_3^j - x_2)}{y_{23}\cos(\theta_{23} - \alpha_{23})}.
\end{aligned}
\qquad (12)
$$

If we denote $R = \alpha, \theta, x, y$, we have $R_{13} = (R_1 + R_3^{j-1})/2$ and $R_{23} = (R_2 + R_3^{j-1})/2$. At the initial iteration, it is assumed that $R_3^0 = (R_1 + R_2)/2$. The relations on axis θ=0 and y=0, and those on the wall, $\tan(\theta) = f'(x)$ and $y = f(x)$ are considered. System (12) was solved by iteration until the conditions $\max\left|R_3^j - R_3^{j-1}\right| < 10^{-8}$ was satisfied. Thus, the known characteristic C_i^+ was used to compute the next characteristic C_{i+1}^+ starting from the axis toward the wall (Figure 7).

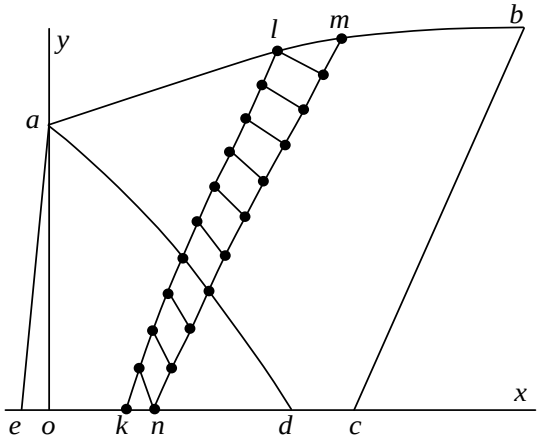

Figure 7. Nozzle computation by the method of characteristic: *oa* – minimum cross section, *ab* – nozzle with a corner point, *ad* – characteristic C^- possessed by the rarefaction wave, *ae* – initial characteristic C_0^+, *kl* – characteristic C_i^+, *nm* – characteristic C_{i+1}^+, *cd* – characteristic C^+.

Here, i and i+1 are the indices of the computed characteristics. Then, the computations were continued until the computed characteristic C^+ comes to the point *b*. The inlet boundary conditions were the initial uniform characteristic C_0^+ (a straightforward line *ae* in

Figure 7) with $\theta_{in}=0$ and $M_{in}=1.001$, where *in* corresponds to the nozzle inlet. Comparison with the boundary conditions $\theta_{in}=0$ and $M_{in}=1$, in the form of a straightforward sonic line from which deviation is realized [15], shows that this replacement scarcely affects the final result, and, hence, the inlet boundary conditions in the McCormack scheme are specified as $\theta_{in}=0$ and $M_{in}=1.001$ on the straightforward line *ao* (Figure 7).

The computation along the characteristic C^+ is convenient, because the computation algorithms for a smooth nozzle and for a corner-point nozzle differ only by the node arrangement on the initial characteristic C_0^+. For a smooth nozzle, the node coordinates were set with a constant step, while for a nozzle with a corner, some of the nodes were set with a constant step and the others were placed at the corner point. The abscissas of the nodes at the corner point were zero, the ordinates were equal to unity, and the values of α and θ were found by Prandtl – Meyer formula (5) with a constant step in α.

In some cases, computations were performed along the characteristic C^-. However, the basis for the algorithm was also the iteration solution of the nonlinear system of equations (12).

In problem *b*, the type of equations (1) change from elliptical to hyperbolic in going from the subsonic to supersonic flow. Therefore, the problem was solved by the second-order-accuracy iteration method proposed in [18]. The method uses the new coordinates ψ and φ, where ψ is the streamline and φ is its orthogonal complement, and the new dependent variable θ, $z=M^2$, S, and H. Elimination of the mixed derivatives by cross differentiation gives the second-order equations:

$$\begin{aligned}
&\frac{\partial}{\partial\psi}\left(K_1\frac{\partial\theta}{\partial\psi}\right)+\frac{\partial}{\partial\varphi}\left((1-z)L_1\frac{\partial\theta}{\partial\varphi}\right)+\frac{\partial K_2}{\partial\psi}+\frac{\partial}{\partial\varphi}((1-z)L_2)=0,\\
&\frac{\partial}{\partial\psi}\left(\frac{1}{L_1}\frac{\partial z}{\partial\psi}\right)+\frac{\partial}{\partial\varphi}\left(\frac{(1-z)}{K_1}\frac{\partial z}{\partial\varphi}\right)-\frac{\partial}{\partial\psi}\left(\frac{L_2}{L_1}\right)+\frac{\partial}{\partial\varphi}\left(\frac{K_2}{K_1}\right)=0,
\end{aligned} \tag{13}$$

where K_1, K_2, L_1, and L_2 are combinations of dependent and independent variables [19]. For S and H, we have the first-order equations on the basis of which (2) is:

$$\frac{\partial H}{\partial\varphi}=0,\quad \frac{\partial S}{\partial\varphi}=0.$$

For determination of θ and z, each of the equations (13) was solved by the approximate factorization method. Since the computation was completed in the supersonic region, the exit boundary conditions were not needed. The inlet boundary conditions are $\theta=0$. If A_{ij} and B_{ij} are the residuals of the difference counterparts of (13) in the grid nodes, and N_1 and N_2 are the number of grid points in φ and ψ, then the iteration continued until the condition:

$$\max\left(\sum_{i}^{N_1}\sum_{j}^{N_2}\frac{|A_{ij}|}{N_1N_2},\sum_{i}^{N_1}\sum_{j}^{N_2}\frac{|B_{ij}|}{N_1N_2}\right)<10^{-8}$$

was satisfied. This method was used in direct computations because, compared with the relaxation method, it is at least an order of magnitude faster [19].

4. CHOICE OF THE FUNCTIONAL

Gas dynamics problems solved by a direct method require construction of a functional with a minimum in the optimum solution. Moreover, an optimum solution, as a rule, must satisfy certain conditions. We consider only the simplest equality-type geometric conditions, primarily dimensional ones where points through which the contour of the desired nozzle passes with a specified slope are set. These geometric conditions are rather easy to realize in the nozzle contour approximation. Using appropriate approximations, it is possible, though more difficult, to take into account inequality-type geometric conditions, e.g. the requirement on a positive ($f'(x)\geq 0$) or negative ($f'(x)\leq 0$) slope of the nozzle profile. Some conditions, e.g. the inadmissibility of the intersection of characteristics of one family in the supersonic region or the existence of a single sonic line in the transonic region, are sometimes difficult to satisfy automatically. The above conditions are normally implicit in the functional. Moreover, certain constraints arise from analyzing the computation results and necessitate heuristic procedures for their consideration. As an example, we refer to the model problems to demonstrate how the functional is constructed.

Problem *a*. Note that M_0 used in the problem is determined from the transcendental equation:

$$y_b{}^2=\frac{M_{in}}{M_0}\left(\frac{2+(\gamma-1)M_0{}^2}{2+(\gamma-1)M_{in}{}^2}\right)^{\frac{\gamma+1}{2(\gamma-1)}},$$

derived from (6) taking into account that $y_a=1$.

Two situations may occur in the direct computation (Figure 7):

(1) A normal situation in which the computation reaches the characteristic C^+=*cb*. In this case, the direct computation is completed by computing the functional. Because the problem conditions include the requirements on *cb* (8), the functional is computed using the parameters on this characteristic.

(2) A controllable abnormal end (or simply an abend) in which a negative slope of the nozzle contour appears or the computation of the next characteristic C^+_{i+1} involves the intersection of characteristics of one family. In this case, the direct computation

stops, and the functional is computed along the last-calculated characteristic C_i^+ to provide a simple connected domain of the functional.

Let there be an optimum nozzle for which direct computation runs to completion and we can accurately predict the functional behavior. Taking into account the foregoing situations, we consider two functionals computed along an arbitrary C_i^+ in this nozzle:

$$J_1 = \sqrt{\frac{1}{L}\int_{C_i^+} \theta^2 dl},$$

$$J_2 = \sqrt{\frac{1}{L}\int_{C_i^+} ((\alpha - \alpha_0)/\alpha_{in})^2 dl},$$

where, $L = \int_{C_i^+} dl$ is the length of C_i^+, $\alpha_{in} = \arcsin(1/M_{in})$, $\alpha_0 = \arcsin(1/M_0)$, and dl is a element of C_i^+.

It is seen from consistency condition (4) that J_1 has two minima, and equals to zero. The first minimum corresponds to the characteristic *ae* with $\theta=0$ and $\alpha=\alpha_{in}$, and the second minimum to *cb* with $\theta=0$ and $\alpha=\alpha_0$. Apparently, only the second minimum is a necessary and sufficient condition for the problem solving. Therefore, the first functional fails to ensure the uniqueness of the solution and, as shown by computations, the resulting solution depends on the initial approximation of the nozzle contour.

Unlike J_1, the functional J_2 has one minimum, and equals to zero on *cb* with $\alpha=\alpha_0$. However, this minimum, though necessary, is an insufficient condition for the problem solving, since we may have that $\theta\neq 0$.

A combination of J_1 and J_2 gives the functional:

$$J_3 = \sqrt{\frac{1}{L}\int_{C_i^+} \left[((\alpha - \alpha_0)/\alpha_{in})^2 + \theta^2\right] dl}.$$

This functional has one zero minimum on *cb* with $\theta = 0$ and $\alpha = \alpha_0$. Hence, this minimum is a necessary and sufficient condition for the problem solving. Thus, the constructed functional J_3 must provide the required result.

However, in practice, it was not the case! During the optimization, contours with negative slopes $f'(x)<0$ appeared. Sometimes, the situation involved an additional local minimum of the functional and the minimum search program considered it as the final result and the end of running. Naturally, the resulting contour in this case did not fit to conditions (8). A way out was found by introducing one more term into the functional. The term calculated the area of sections with a negative slope, and the functional took the following form:

$$J = \sqrt{\frac{1}{L}\int_{C_i^+}\left[\left((\alpha-\alpha_0)/\alpha_{in}\right)^2+\theta^2\right]dl} + \int_{x_a}^{x_b}\varphi_0(x)dx \quad (14)$$

with

$$\varphi_0(x) = \begin{cases} |f(x)|, & f'(x) < 0, \\ 0, & f'(x) \geq 0. \end{cases}$$

If the nozzle has a negative slope $f'(x_a) < 0$ at the initial point, an abend occurs during the computation of C_1^+ and the functional is calculated on the initial characteristic $C_0^+ = ae$. Because, Prandtl-Meyer formula (5) is used at the corner point, it can also be used at $\theta_2 < 0$, as shown in Figure 8.

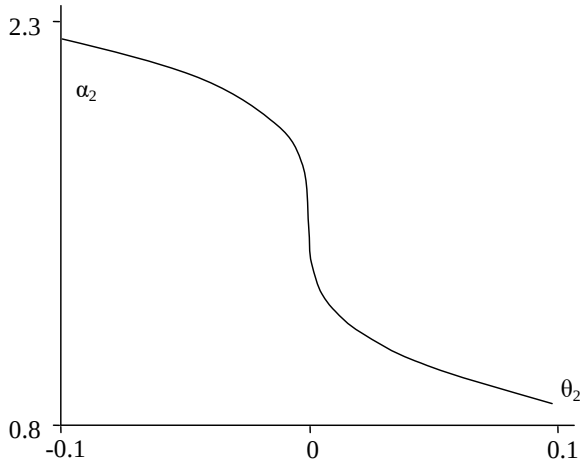

Figure 8. Dependence of α_2 on θ_2 for γ=1.4, $\alpha_1=\pi/2$ and θ_1=0 in Prandtl–Meyer formula (5).

In this case, the determined values of α have no physical meaning, since the rarefaction wave is absent. However, for a negative nozzle slope at the initial point, formula (5), due to its continuity, makes it possible to continue the functional toward the simple connected domain and, thus, to provide the functional continuity.

Further, computations show that functional (14) ensures the desired result.

Problem *b*. Initially, this problem used the functional:

$$J = \int_{M=1}|y|dx + \int_{-2}^{0}\varphi_1(x)dx \qquad (15)$$

with

$$\varphi_1(x) = \begin{cases} |f(x)|, & f'(x) > 0, \\ 0, & f'(x) \le 0. \end{cases}$$

The first integral was calculated along the line M=1 and was numerically equal to the area between the line M=1 and straightforward line x=0. The last term is equal to the area under the curve for the nozzle part with a positive slope. Apparently, this functional has a minimum in the case of a plane sonic line in the minimum cross section and a monotonic nozzle profile, which was confirmed by numerical studies. However, analysis of the results showed that, in some cases, there was a local supersonic region on the wall (Figure 9). The Mach number inside this region reached 1.3 and, in passing though the right boundary, it becomes subsonic, which must involve the initiation of a shock wave. Obviously, condition (2) used in realizing the method [18] is not satisfied in this case; the flow is nonpotential and the resulting solution does not fit the physics of the process. This conclusion was confirmed by computation according to complete system (1) using the relaxation method in combination with both Godunov and McCormack schemes. This computation revealed only one sonic line (Figure 9).

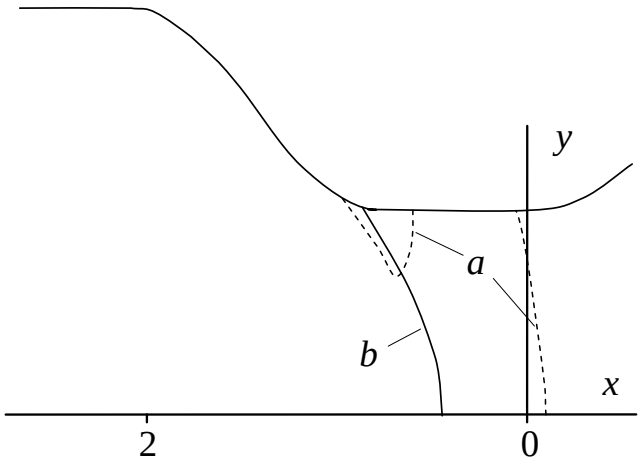

Figure 9. Sonic line position in problem *b* in different statements: (*a*) potential flow and two lines M=1 inadequate for the physics of the process, (*b*) nonpotential flow and one line M=1.

Therefore, to avoid contours with local supersonic regions, functional (15) was supplemented with the term:

$$J = \int_{M=1} |y| dx + \int_{-2}^{0} \varphi_1(x) dx + \int_{x=-2.5}^{x=0} \varphi_2(l) dl \quad (16)$$

with

$$\varphi_2(l) = \begin{cases} 1, & \partial M / \partial l > 0, \\ 0, & \partial M / \partial l \le 0, \end{cases}$$

where l is a element of the nozzle contour length and the function $\varphi_2(l)$ is computed on the nozzle wall. The last term in (16) is equal to the length of a nozzle part with a positive gradient of the Mach number. Functional (16) made possible solutions with no local supersonic regions and contours with near-plane sonic lines.

5. NOZZLE DESCRIPTIONS

As noted above, direct computation may, sometimes, comes to an abend due to a poor nozzle shape generated by the minimum search procedure. The poor shape implies violation of the supersonic or subsonic part monotonicity downstream and upstream of the minimum cross section, respectively. Obviously, the nozzle profile monotonicity is a necessary, but insufficient condition for normal completion of direct computation. Moreover, the efficiency of direct computations depends heavily on the choice of nozzle contour approximations. If the type of the hypersurface $J(c_1,\ldots,c_N)$ is near quadratic, the minimum search procedure for a function of many variables [5] finds the minimum in direct runs which number is proportional to N^2. In [17] and [20], it is shown that monotone approximations decrease the number of abends and increase the direct method performance.

Unfortunately, an approximation suitable for any problem is yet unknown, and we use monotone and nonmonotone methods of nozzle contour description.

5.1. Problem *a.* Nozzle Description Using Basis Functions

First, we consider approximations of the desired supersonic nozzle $f(x)$ in the form of expansions in terms of certain bases. A more detailed description of the procedure can be found in [17]. The number of varied (independent) parameters in each approximation is denoted as N. Each item begins with brief notation of the underlying method.

$P(c)$. The basis functions are the power polynomials:

$$f(x)=\sum_i c_i t^{i-1}, \quad t=(x-x_a)/(x_b-x_a).$$

$CH(c)$. The expansion is constructed in terms of the Chebyshev polynomials of the first kind $T_i(t)$:

$$f(x)=\sum_i c_i T_i(t), \quad t=(2x-x_b-x_a)/(x_b-x_a).$$

Because geometric conditions must be fulfilled (7), three coefficients are expressed in terms of the others through $P(c)$ and $CH(c)$. For the number of independent parameters c_i to be N, we should use N+3 basis functions.

$B2m(c)$. The interval $[x_a, x_b]$ is divided into k subintervals $x_i=x_a+ih$, $i=0,1,\ldots,k$, where, $h=(x_b-x_a)/k$. The function $f(x)$ is represented as an expansion in terms of quadratic B-splines $B_2(x)$ ([17]):

$$f(x)=\sum_i a_i B_2(x-x_i)\,. \qquad (17)$$

The support of $B_2(x)$ occupies only three subintervals and the desired function $f(x)$ for $x\in[x_i,x_{i+1}]$ is expressed via only three terms of the sum in (17):

$$f(x)=[a_{i-1}(1-t)^2+a_i\big(1+2t(1-t)\big)+a_{i+1}t^2]/2,\quad t=(x-x_i)/h\,. \qquad (18)$$

A sufficient condition for spline (17) to increase and be nonnegative on the interval $[x_a,x_b]$ is the monotonicity of the sequence of coefficients $a_{-1},a_0,\ldots,a_k$ [21]:

$$0\le\ldots\le a_{i-1}\le a_i\le a_{i+1}\ldots.$$

Assume that the expansion coefficients a_i are related by [22]:

$$a_i=a_{i+1}+(a_{i-1}-a_{i+1})\sin^2(c_{i+1}+\pi/4)\,.$$

Then, for any set of c_i, the expansion coefficients in (17) always form a monotone sequence. Taking into account geometric conditions (7), we obtain a tridiagonal system of linear equations for determining the spline coefficients $a_{-1},\ldots,a_k$:

$$\begin{cases} a_{-1}+a_0=2y_a,\\ a_{i-1}\sin^2(c_{i+1}+\pi/4)-a_i+a_{i+1}\cos^2(c_{i+1}+\pi/4)=0,\quad i=0,\ldots,k-2,\\ a_{k-1}+a_k=2y_b,\\ -a_{k-1}+a_k=hy_b'. \end{cases} \qquad (19)$$

Thus, with quadratic *B*-splines, the computations are organized as follows: setting the number $N>0$ and the independent variables $c_{-1},\ldots,c_N$; dividing the interval $[x_a,x_b]$ into $k=N+1$ equal subintervals; determining $a_{-1},\ldots,a_k$ from system (19), and for a given abscissa x, calculating the ordinate of the nozzle contour $f(x)$ by formula (18).

*B*3*m*(*c*). Using the previous notions, the function $f(x)$ is represented as an expansion in terms of the cubic *B*–splines $B_3(x)$ ([17]):

$$f(x)=\sum_i a_i B_3(x-x_i)\,.$$

For $x\in[x_i,x_{i+1}]$, only four terms are nonzero and $f(x)$ takes the form:

$$f(x)=[a_{i-1}(1-t)^3+a_i(4-3t+3t(1-t)^2)+a_{i+1}(1+3t+3t^2(1-t))+a_{i+2}t^3]/6\,.$$

The order of computations and the monotonicity property are the same as with quadratic splines. However, the basis functions, the number of expansion coefficients $a_{-1},\ldots,a_{k+1}$ and the number of divisions $k=N$ are different. The system of linear equations (19) is replaced with:

$$\begin{cases} a_{-1}+4a_0+a_1=6y_a, \\ a_{i-1}\sin^2(c_{i+1}+\pi/4)-a_i+a_{i+1}\cos^2(c_{i+1}+\pi/4)=0, \quad i=0,\ldots,k-1, \\ a_{k-1}+4a_k+a_{k+1}=6y_b, \\ -a_{k-1}+a_{k+1}=2hy'_b. \end{cases}$$

It should be emphasized that only the formulae in $B2m(c)$ and $B3m(c)$ imply that $f(x)$ is monotonic for any values of $c_{-1},\ldots,c_N$; hence $\varphi_0(x)=0$ in (14).

5.2. Problem *a*. Nozzle Description Using Interpolants

The desired supersonic contour is described by interpolants satisfying condition (7) and passing through certain points (x_i,y_i), where $y_i\in[y_a,y_b]$. Some of y_i can be given. The values of x_i are given on a uniform grid. In this section, we consider only two given points *a* and *b*, but their number can easily be increased. In what follows, except as otherwise noted, we use the following notations:

$$y_0=y_a, \quad y_N=y_b, \quad x_i=x_a+ih, \quad i=0,1,\ldots,N, \quad h=(x_a-x_b)/N,$$

$x\in[x_i,x_{i+1}]$, and $t=(x-x_i)/h$. The values of y_i are specified using arbitrary linearly independent parameters $c_1,\ldots,c_N$. Each item begins with brief notation of the underlying method.

S(y). The interpolant is a cubic spline of the class C^2 [23] that is a cubic polynomial on each subinterval $[x_i,x_{i+1}]$:

$$f(x)=y_i(1-t)+y_{i+1}t+h[u_i(1-t)((1-t)^2-1)+u_{i+1}t(t^2-1)]. \qquad (20)$$

The values of u_i are found from the system of linear equations:

$$\begin{cases} 2u_0+u_1=(y_1-y_0)/h-y'_0, \\ u_{i-1}+4u_i+u_{i+1}=(y_{i+1}-2y_i+y_{i-1})/h, \quad i=1,\ldots,N-1, \\ u_{N-1}+2u_N=y'_b-(y_N-y_{N-1})/h, \end{cases} \qquad (21)$$

in terms of $y_1,\ldots,y_{N-1}$ and y'_0, which are specified as:

$$y_0' = (0.1 + c_1)^2, \qquad (22)$$

$$y_i = y_a + \sin^2(c_{i+1} + \pi/4)(y_b - y_a), \quad i = 1,\ldots,N-1. \quad (23)$$

Formulae (22) and (23) are required to ensure that $y_0' \geq 0$ and $y_a \leq y_i \leq y_b$, respectively.

S(*ym*). The interpolant is again a cubic spline satisfying (20) – (22), but formulae (23) are replaced with:

$$y_i = y_{i-1} + \sin^2(c_{i+1} + \pi/4)(y_{i+1} - y_{i-1}), \quad i = 1,\ldots,N-1, \qquad (24)$$

to provide the monotonicity of the interpolated values: $y_{i-1} \leq y_i \leq y_{i+1}$. Using the boundary conditions and expressions (24), we obtain the system of linear equations to solve for the unknowns $y_1,\ldots,y_{N-1}$:

$$\begin{cases} y_1 - \sin^2(c_2 + \pi/4)y_2 = \cos^2(c_2 + \pi/4)y_0, \\ -\cos^2(c_{i+1} + \pi/4)y_{i-1} + y_i - \sin^2(c_{i+1} + \pi/4)y_{i+1} = 0, \quad i = 2,\ldots,N-2, \\ -\cos^2(c_N + \pi/4)y_{N-2} + y_{N-1} = \sin^2(c_N + \pi/4)y_N. \end{cases} \qquad (25)$$

It should be noted that although the interpolated values are monotone, the values of *S*(*ym*) between the nodal values of y_i may be nonmonotone.

Sm(*y*). We use the same cubic spline defined by (20) and (21). However, y_i are specified so that not only monotonicity but also the monotonicity of the spline between the nodes is ensured. Sufficient conditions for the cubic spline to be monotone are that the neighboring differences diverge no more than threefold [24]:

$$\frac{1}{3} \leq \frac{y_i - y_{i-1}}{y_{i+1} - y_i} \leq 3, \qquad (26)$$

Moreover, the same is true for the boundary derivatives:

$$\begin{aligned} &0 \leq y_0' \leq 3(y_1 - y_0)/h, \\ &3(y_N - y_{N-1})/h \geq y_N'. \end{aligned} \qquad (27)$$

Expressing y_i in terms of c_i so that inequalities (26) automatically yields:

$$3(y_i - y_{i-1}) = (8\sin^2(c_{i+1}) + 1)(y_{i+1} - y_i).$$

Then, instead of system (25), we have:

$$\begin{cases} y_1(4+8\sin^2(c_2))-y_2(1+8\sin^2(c_2))=3y_0, \\ -3y_{i-1}+y_i(4+8\sin^2(c_{i+1}))-y_{i+1}(1+8\sin^2(c_{i+1}))=0, \quad i=2,...,N-2, \\ -3y_{N-2}+y_{N-1}(4+8\sin^2(c_N))=y_N(1+8\sin^2(c_N)), \end{cases}$$

and, instead of formula (22), in view of (27), we obtain:

$$y'_0=3\sin^2(c_1+\pi/4)(y_1-y_0)/h.$$

Rm(*y*). The interpolant is the rational spline taken from [25]:

$$f(x)=y_i(1-t)+y_{i+1}t+u_i\frac{1-t}{A_i}\left[\frac{(1-t)^2}{1+q_it}-1\right]+u_{i+1}\frac{t}{B_i}\left[\frac{t^2}{1+p_i(1-t)}-1\right],$$

where $A_i=\left(3+3q_i+q_i^2\right)/h$ and $B_i=\left(3+3p_i+p_i^2\right)/h$. The values of y'_0 and y_i are determined by formulae (22) and (25), and those of u_i from the system of linear equations:

$$\begin{cases} \dfrac{2+q_0}{A_0}u_0+\dfrac{u_1}{B_0}=y_1-y_0-h\,y'_0, \\ \dfrac{u_{i-1}}{A_{i-1}}+\left(\dfrac{2+q_i}{A_i}+\dfrac{2+p_{i-1}}{B_{i-1}}\right)u_i+\dfrac{u_{i+1}}{B_i}=y_{i+1}-2y_i+y_{i-1}, \quad i=1,\ldots,N-1 \\ \dfrac{u_{N-1}}{A_{N-1}}+\dfrac{2+p_{N-1}}{B_{N-1}}u_N=h\,y'_N-y_N+y_{N-1}. \end{cases}$$

For the rational splines to be always monotone for monotone y_i, it is sufficient to determine the control parameters p_i and q_i from the relations [24]:

$$q_0=\max\left[0,\frac{3}{2}\frac{y'_0}{(y_1-y_0)/h}-3\right],$$

$$q_i=\max\left[0,\frac{3}{2}\frac{y_i-y_{i-1}}{y_{i+1}-y_i}-3\right], \quad i=1,\ldots,N-1,$$

$$p_{i-1}=\max\left[0,\frac{3}{2}\frac{y_{i+1}-y_i}{y_i-y_{i-1}}-3\right], \quad i=1,\ldots,N-1,$$

$$p_{N-1} = \max\left[0, \frac{3}{2}\frac{y'_N}{(y_N - y_{N-1})/h} - 3\right].$$

P(y). The values of y'_0 and y_i are given by (22) and (23), and conditions (7) are taken into account using the interpolation polynomial:

$$f(x) = \sum_i c_i t^{i-1}, \quad t = \left(2x - x_a - x_b\right)/\left(x_b - x_a\right). \quad (28)$$

P(ym). The interpolation polynomial is again given by (28), but y_i are determined not from (23) but from (25), which ensures the monotonicity of these values. Naturally, these values of $P(ym)$ between the nodes may be nonmonotone.

Note that the complete monotonicity of $f(x)$ is ensured only by $Sm(y)$ and $Rm(y)$ with $\varphi_0(x) = 0$ in (14).

5.3. Problem *b*. Nozzle Description

The subsonic nozzle part is described using all interpolants and all basis functions, except for the quadratic *B*–splines, since the continuity of the corner up to the second derivative is required for solving equations (13) on the nozzle wall $f(x)$. Compared with (10) in problem *a*, geometrical conditions (7) involve one more derivative. Considering that the additional condition is obvious and, for this reason, is not discussed.

Thus, for all descriptions considered above, the nozzle profile $f(x)$ depends on N linearly independent coefficients $c_1,\ldots,c_N$. Hence, the problem on the nozzle profile $f(x)$ that minimizes the functional J is reduced to a search for a point $(c_1,\ldots,c_N)$ at which the function of many variables $J(c_1,\ldots,c_N)$ has a minimum.

5.4. Numerical Results

In problem *a*, the computations were performed for x_b=3.576 and y_b=1.299 and taken from the reference problem. The number N of varied variables was between 1 and 10. The initial value of c_i, in all cases, was zero, which corresponds to an initial approximation in the form of a nozzle with no corner point for all the basis functions and for the interpolants $P(y)$, $P(ym)$. Fifty points were specified on the characteristic *ae*. The resulting nozzle was compared with the reference profile computed by the procedure described in [15]. The reference nozzle was a nozzle with a corner point from the family $W(\gamma,M_0,G)$, with γ=1.4, M_0=2, G=1.

Table 1 and Table 2 demonstrate how the number of coefficients and the method of nozzle description affect the minimization results. The functional values / the number of direct runs / the number of abends are presented in Table 1 and Table 2.

For the basis functions, the values of functionals decrease monotonically with increasing N, and the Chebyshev polynomials $CH(c)$ are slightly superior. However, unlike [4], with a

fixed *N*, the Chebyshev polynomials have no clear advantages for the number of direct runs and abends. With interpolants, a monotonic decrease in values of functionals with increasing *N* was found only for the monotone rational spline *Rm*(*y*). For *S*(*ym*), *Sm*(*y*) and *P*(*ym*), this monotonicity is somewhat violated with large *N*; however, we can see that a priory information on the monotonicity of the points is advantageous over the ordinary representation for *S*(*y*) and *P*(*y*) in which increasing *N* scarcely improves the result.

Table 1. Problem *a*: nozzle description via basis functions

N	*B2m*(*c*)	*B3m*(*c*)	*CH*(*c*)	*P*(*c*)
1	23.1/11/0	24.5/12/0	22.1/17/3	22.1/12/0
2	12.7/26/0	7.6/33/0	5.9/37/5	5.9/58/1
3	8.5/49/0	3.8/56/0	2.5/73/8	2.5/102/1
4	6.1/81/0	2.5/86/0	1.5/95/9	2.3/102/1
5	4.6/110/0	1.8/135/0	1.1/142/13	2.0/102/1
6	3.6/160/0	1.4/164/0	0.9/205/14	1.8/102/1
7	2.9/181/0	1.1/221/1	0.8/244/16	1.8/236/2
8	2.3/221/0	1.0/278/0	0.8/269/20	1.7/283/2
9	1.9/280/0	0.9/336/0	0.8/294/22	1.5/444/2
10	1.6/339/0	0.8/371/0	0.8/346/25	1.5/457/2

Table 2. Problem *a*: nozzle description via interpolants

N	*S*(*y*)	*S*(*ym*)	*Sm*(*y*)	*Rm*(*y*)	*P*(*y*)	*P*(*ym*)
1	22.1/14/0	22.1/14/0	22.1/10/0	22.1/14/0	22.1/14/0	22.1/14/0
2	7.6/41/0	7.6/41/0	11.4/55/0	7.2/41/0	5.9/42/0	5.9/42/0
3	3.8/213/2	3.8/63/0	6.9/67/0	5.0/61/0	2.5/66/0	2.5/64/0
4	2.5/283/17	2.5/88/0	4.2/101/0	2.9/93/0	1.5/119/1	1.5/121/0
5	1.8/634/4	1.8/147/0	2.7/160/0	2.1/134/0	177.5/54/3	1.1/155/0
6	1.4/253/1	1.4/200/0	2.0/233/0	1.6/173/0	93.5/247/3	0.9/231/1
7	142.8/702/12	1.1/216/1	1.5/268/0	1.2/290/0	229.6/181/14	0.8/288/0
8	153.6/507/5	1.0/251/2	1.2/331/9	1.0/293/1	191.0/345/42	0.8/288/0
9	247.8/141/22	0.9/342/0	99.1/442/0	0.9/301/1	185/178/27	4.1/287/0
10	265.8/290/21	36.9/1025/1	8.0/297/0	0.8/381/0	305.2/199/47	0.8/516/5

A priory monotonicity information exerts a much stronger effect on the number of abends during the optimization. The number of direct runs depends largely on the number of varied variables, and with a priory monotonicity information, the number of abends may decrease by an order of magnitude. For basis functions, the largest number of abends was observed with *CH*(*c*), no abend with *B*2*m*(*c*), one abend with *B*3*m*(*c*), and several abends with *P*(*c*). Similar results were obtained with interpolants. In the approximations of *S*(*y*) and *P*(*y*) without considering the monotonicity information on the interpolated data, the number of abends is very large, whereas applying the monotonicity information (*Rm*(*y*), *Sm*(*y*), *S*(*ym*) and *P*(*ym*)), only a few abends occur.

It should be noted that for each method used in problem *a*, computed nozzle ordinates at the point of the functional minimum differ from the ordinate of the reference one by less than 10^{-3} (Table 1, Table 2 and Figure 10).

Moreover, the result profile in all the cases was a nozzle with a corner point. As an illustration, Figure 1 shows the initial, final, and several intermediate nozzle profiles obtained in iterations of the functional minimization with the initial smooth profile.

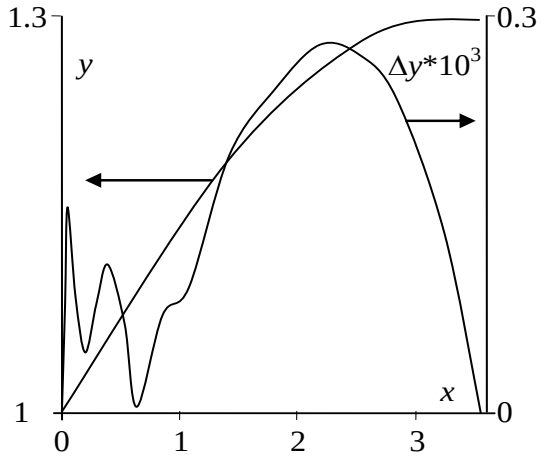

Figure 10. Results of supersonic nozzle optimization in the basis of *B*-splines *B*3*m*(*c*) for *N*=10: *y* - nozzle obtained by direct computation, Δ*y* – modulus of difference between the obtained and reference nozzles.

Table 3. Problem *b*: nozzle description via basis functions

N	***B3m*(*c*)**	***CH*(*c*)**	***P*(*c*)**
1	195.0/21/0	208.7/33/11	211.9/40/0
2	34.4/147/0	207.8/68/23	-
3	20.2/183/0	208.6/76/29	-
4	21.0/253/0	213.3/77/29	-
5	18.7/245/0	-	-

Table 4. Problem *b*: nozzle description via interpolants

N	***S*(*y*)**	***S*(*ym*)**	***Sm*(*y*)**	***Rm*(*y*)**	***P*(*y*)**	***P*(*ym*)**
1	198.4/29/4	198.4/29/4	198.4/16/0	254.3/1/0	208.7/18/2	208.7/18/2
2	-	34.5/141/7	223/108/0	55.4/161/0	-	76.1/111/15
3	166.2/239/25	19.9/245/19	75.1/105/0	51.6/171/0	-	78.9/258/36
4	229.7/161/80	21.0/190/16	58.8/188/0	33.6/345/0	-	91.4/125/17
5	-	19.7/209/16	38.8/611/0	29.1/25/0	-	102.7/397/100

In problem *b*, the number *N* of varied variables was changed from 1 to 5, and the initial value of c_i, in all cases, was zero. Equation (4) was solved, using a 40 × 40 grid. In Table 3 and Table 4 the functional values / the number of direct runs / the number of contours with a negative slope for problem *b* are presented. Here, $f'(x) > 0$ corresponds to oscillatory contour variations near the minimum cross section. The sign "-" in a table cell means that the

computation has failed (an explanation is given in the next section). In problem *b*, the advantage of the approximations *B*3*m*(*c*), *S*(*ym*), *Sm*(*y*), *Rm*(*y*), and *P*(*ym*), which use in one way or another a priory nozzle monotonicity information, is even more evident. It is seen from Table 3 and Table 4 that the minimum value of functional was obtained for *B*3*m*(*c*). The presented results clearly indicate that in this problem, *B*3*m*(*c*), *Sm*(*y*), and *Rm*(*y*) are preferable, i.e. the problem is hardly solved without priory monotonicity information.

Figure 11 shows contours and corresponding positions of sonic lines obtained for problem *b*. The results for $N = 4$ are not shown, since they lie between $N = 3$ and $N = 5$.

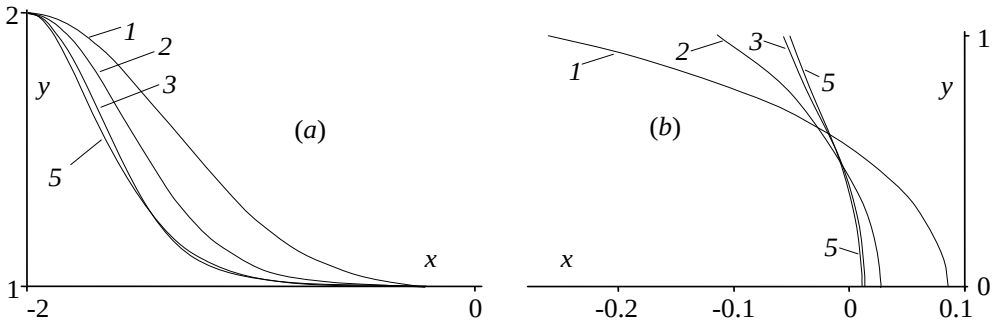

Figure 11. Results of subsonic nozzle optimization in the basis of *B*-splines *B*3*m*(*c*): *1*, *2*, *3* and *5* – number of varied coefficients; (*a*) nozzle profile; (*b*) line M=1.

5.5. Troubles and Ways Around

It is seen in Table 3 and Table 4 that we failed to derive some solutions to problem *b*. The fact is that in some cases, where a positive-slope contour is obtained at the first step, functional (16) results in a local minimum at which the minimum search program stops. In other cases, an abend occurs inside the iteration method at intermediate optimization steps [18] due to the specific nozzle shape. There are several ways of solving these problems:

(1) Use methods less responsive to local minima, e.g. the Monte-Carlo method or genetic algorithms rather than the minimum search procedure based on Broyden quasi-Newton method [5]; however, these methods are slow.
(2) Replace the iteration method [19] with the relaxation method based on Godunov scheme, capable of computing the flow in virtually all contours; then, functional (16) is simplified to involve only first term, but the time of direct computation may become too long.
(3) More thoroughly analysis of the nozzle profile before beginning the direct computation provides more stable performance of the iteration method [18]. In this case, one should somehow change functional (16) and introduce a procedure of analyzing the nozzle profile.
(4) Use another method of nozzle profile description, e.g. nonuniform-grid splines.

6. WIND TUNNEL DESIGN

6.1. Problem Statement and Solving Procedures

To reduce the time of wind tunnel designs with different exit Mach numbers M_0, the authors of [26] suggested designing the supersonic nozzle of a wind tunnel as a combination of its fixed part and changeable part adjacent to the minimum cross section. A similar design is considered in [27] with the changeable part shape calculated by direct methods and the nozzle approximated by splines. In [28], it is proposed to select the changeable part on the set $W(\gamma,M_0,G)$. So, not the entire contour is used, but only part of the contour is smoothly linked up with the fixed nozzle profile. The fixed part was also chosen from $W(\gamma,M_0,G)$. Note that, unlike problem *a*, the nozzle profile of a wind tunnel, in this case, has no corner point.

In [6], it was proposed to compute this wind tunnel by a two-step direct method. The first step is made within the ideal gas model and, because of the necessity to account for viscosity in supersonic nozzles [29], the result solution is used as the initial approximation in the viscous problem at the second step. Let's consider only the contour design in the ideal gas model. The Mach numbers to be realized at the wind tunnel exit for k changeable parts are expressed in terms of $M_{0k} <\ldots< M_{02} < M_{01}$. We restrict ourselves to the simplest case, where, k=2. The nozzle design consisting of a fixed part db, a changeable part a_1d with M_{01}=20, and a changeable part with M_{02}=14 is proposed to be as follows (Figure 12):

(1) A nozzle a_1b with uniform characteristic c_1b and M_{01} at the exit is designed by the method of characteristics.
(2) The changeable nozzle part for M_{01} and the fixed part are defined. For this purpose, given nozzle contour a_1b, a uniform characteristic c_2b is constructed from M_{02}. Then, the method of characteristics is used to compute the flow parameters between the given nozzle contour a_1b and the characteristic c_2b until dc_2 issuing from the axis is obtained. This procedure indicates the changeable part a_1d for M_{01} and the fixed part db. Apparently, the resulting length of db is minimum.
(3) And the changeable nozzle part a_2d is designed for M_{02} using a nozzle approximation similar to that used in problem *a*, excluding the fact that geometric conditions (7) take the form:

$$f(x_a)=1, \qquad f'(x_a)=0, \qquad x_a=0,$$

$$f(x_d)=y_d, \qquad f'(x_d)=y'_d,$$

where x_d, y_d, y'_d are taken from the nozzle contour. The changeable part a_2d can be designed using four algorithms.

Algorithm *1*. Direct computation using the part of the contours from $W(\gamma,M_0,G)$, which is smoothly linked up with the fixed profile part. The optimization parameters are γ, M_0, and G with $\gamma > 1$, $M_0 > 1$, and $G \in (0,1]$. Once the contour is found, the flow is computed, and dc_2 is constructed from the plane sonic line. The functional $J(\gamma,M_0,G)$ is the value of area between the known dc_2 and constructed dc_2.

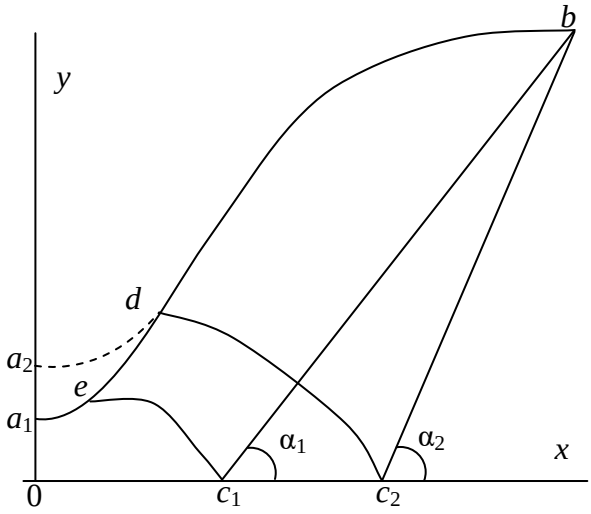

Figure 12. Schematic of a multimode wind tunnel nozzle: a_1d - changeable nozzle part for M_{01}, a_2d - changeable nozzle part for M_{02}, db - fixed nozzle part, dc_2 - determined characteristic C^-, ec_1 - characteristic C^- closing the rarefaction, c_1b - uniform characteristic C^+ with M_{01}, c_2b - uniform characteristic C^+ with M_{02}, $\alpha_1 = \arcsin(1/M_{01})$, $\alpha_2 = \arcsin(1/M_{02})$.

Algorithm *2*. Direct computation is similar to that described for problem *a* and is based on the method of characteristics (12).

Algorithm *3*. Direct computation is similar to that described for problem *a* and is based on McCormack scheme (11).

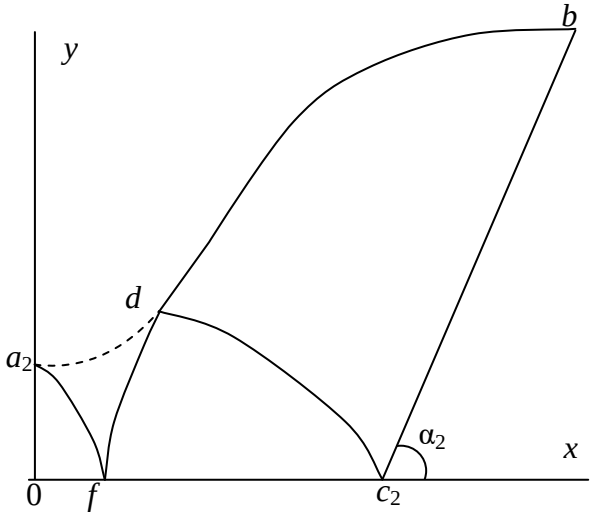

Figure 13. Computation of the changeable nozzle part of a wind tunnel: a_2d – changeable part for M_{02}, db – fixed part, dc_2 – determined characteristic C^-, df - characteristic C^+, a_2f - characteristic C^-, c_2b – uniform characteristic C^+ with M_{02}, $\alpha_2 = \arcsin(1/M_{02})$.

Algorithm *4*. If there is a_2d that provides an accurate uniform c_2b or conditions (8), this contour can be constructed without resort to direct computations (Figure 13), as suggested by

A. N. Kraiko. For this purpose, the parameters between the constructed characteristic dc_2 and the axis are calculated until fd is obtained, by the method of characteristics. At point f, we have M_f. Further, the changeable part a_2d is calculated from the plane sonic line, the characteristics in the rarefaction wave are calculated until M_f is reached on the axis, and the Goursat problem between the calculated characteristic a_2f and the characteristic fd is solved.

Note that the first three algorithms do not require the existence of the contour a_2d that provides accurate fulfillment of conditions (8), since the direct method always constructs the contour a_2d, but conditions (8) are satisfied approximately. Therefore, we used algorithms based on the direct method. However, the algorithms revealed two main problems.

6.2. Problems

Computations show that in direct computation, it is undesirable to run the first step with no abend. To accomplish this in problem *a*, it was sufficient to set the initial approximation in the form of zero values of the control parameters $c_1,\ldots, c_N$. For wind tunnel optimization, these actions were found to be ineffective. Therefore, firstly, we used algorithm *1* and constructed an initial approximation in the form of a contour from the family $W(\gamma,M_0,G)$. The control parameters $c_1,\ldots, c_N$ for the corresponding approximation were determined from the resulting contour using the least square method. Then, we employed algorithms *2* or *3*. Because the corner point must be absent to fit specifications and algorithm *3* is faster, we used this algorithm in further computations.

The exit Mach numbers are 14 and 20, and, hence, the next problem is associated with peculiarities of the approximation of long nozzles. Table 5 shows the nozzle length *xb* from the family $W(\gamma,M_0,G)$ for $\gamma = 1.4$, G=1, and different M_0.

Comparison shows that the nozzle length increases 1000 times as the Mach number is increased from 2 to 22. However, even for the longest nozzles, the main change in the slope occurs at $x\in[0,1]$ (Figure 14) and, thus, the methods considered above provide inaccurate description of these contours. For this reason, we used two other methods of nozzle description.

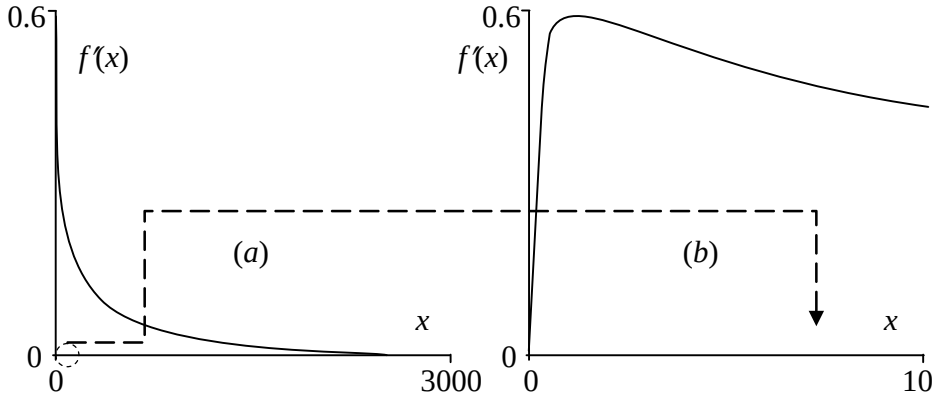

Figure 14. Variation of the slope of a smooth nozzle contour from the family $W(\gamma,M_0,G)$: (*a*) throughout the length, (*b*) on the interval from 0 to 10 (γ=1.4, M_0=20, G=0.81).

Table 5. Nozzle length *xb* versus M_0

M_0	2	4	6	8	10	12	14	16	18	20	22
xb	3.6	16.9	52.3	126.2	258	469.3	784.1	1228.6	1830.5	2619.6	3627.3

6.3. Additional Methods of Nozzle Description

Ln(c). The basis functions are:

$$f(x)=\sum_{i=1} c_i t^{i-1}, \quad t=\frac{\ln(1+x-x_a)}{\ln(1+x_d-x_a)}.$$

Sm(yn). Let's consider a general case, where the contour has a corner point and irregular node arrangement $x_i \in [x_0, x_J]$ and $x_J = x_d$ with specified values y_0, y'_J and $y_N, y_{N+1}, \ldots, y_J$ and variables $y'_0, y_1, \ldots, y_{N-1}$, where J is a number of points. The monotone interpolant is a cubic spline of the class C^2 [23] differing from *Sm(y)* in section 5 by the irregular node arrangement:

$$S_i(x)=\frac{u_i(x-x_{i-1})^3}{h_i}-\frac{u_{i-1}(x-x_i)^3}{h_i}+\left(\frac{y_i}{h_i}-u_i h_i\right)(x-x_{i-1})-\left(\frac{y_{i-1}}{h_i}-u_{i-1}h_i\right)(x-x_i),$$

where $x \in [x_i, x_{i-1}]$, $h_i = x_i - x_{i-1}$, i=1,…,J. The variables u_i are determined from the equations:

$$\begin{cases} 2u_0 h_1 + u_1 h_1 = (y_1 - y_0)/h_1 - y'_0, \\ h_i u_{i-1} + 2(h_i + h_{i+1})u_i + h_{i+1}u_{i+1} = \dfrac{y_{i-1}-y_i}{h_i} - \dfrac{y_i - y_{i+1}}{h_{i+1}}, \quad i = 1,\ldots,J-1, \\ u_{J-1}h_J + u_J h_J = (y_{J-1} - y_J)/h_J + y'_J. \end{cases}$$

The values $y_1,\ldots,y_{N-1}$, y'_0 should be specified so that the spline between the nodes is monotone. Sufficient conditions for this are [24]:

$$\begin{cases} (y_1 - y_0)/h_1 \geq \dfrac{1}{3} y'_0, \\ \dfrac{h_i}{h_{i+1}+2h_i} \leq \dfrac{(y_i - y_{i-1})/h_i}{(y_{i+1}-y_i)/h_{i+1}} \leq \dfrac{h_i + 2h_{i+1}}{h_{i+1}}, \quad i = 1,\ldots,N. \end{cases}$$

For the above conditions to be fulfilled, we proceed to the variables c_i:

$$\begin{cases} y'_0 = 3\sin^2(c_1)(y_1 - y_0)/h_1, \\ \dfrac{(y_i - y_{i-1})/h_i}{(y_{i+1} - y_i)/h_{i+1}} = b_{i+1}, \quad i = 1,\ldots,N, \end{cases}$$

where

$$b_{i+1} = \frac{h_i}{h_{i+1} + 2h_i} + \left(\frac{h_i + 2h_{i+1}}{h_{i+1}} - \frac{h_i}{h_{i+1} + 2h_i} \right) \sin^2(c_{i+1}).$$

The final system of equations for determining $y_{1,\ldots,}y_{N-1}$, y'_0 is:

$$\begin{cases} h_1 y'_0 - y_1 3\sin^2(c_1) = -3\sin^2(c_1) y_0, \\ (h_2 + b_2 h_1) y_1 - b_2 h_1 y_2 = h_2 y_0, \\ h_{i+1} y_{i-1} - (h_{i+1} + b_{i+1} h_i) y_i + b_{i+1} h_i y_{i+1} = 0, \quad i = 2,\ldots,N-1, \\ h_{N+1} y_{N-1} - (h_{N+1} + b_{N+1} h_N) y_N = -b_{N+1} h_N y_{N+1}. \end{cases}$$

Using the determined $y_{1,\ldots,}y_{N-1}$, y'_0 and the known $(x_N, y_N),\ldots,(x_J, y_J)$, y'_J values, we construct a spline. Note that the such obtained values of $y_{1,\ldots,}y_{N-1}$ are not only monotone themselves, but also, provide monotonicity of the spline between the nodes $y_{0,\ldots,}y_N$.

6.4. Computation Results

Direct computation was used to design the changeable nozzle part for a Mach 14 and the fixed nozzle part for a Mach 20. The fixed nozzle part is described by a cubic spline of the class C^2 [23] with irregular node arrangement and a number of points ranging from 3700 to 7500. The changeable profile was described only by $Ln(c)$ with N=10 and $Sm(yn)$ with J=30. The results obtained with other approximations were unsatisfactory. The functional to be minimized was the Mach number distribution nonuniformity in the flow core in the operating region of the wind tunnel [6]. Table 6 demonstrates the advantage of the approximation $Ln(c)$ based on expansion in terms of basis functions in the form the logarithm powers.

Table 6. Method of nozzle description in relation to the result

Description	Flow nonuniformity
$Ln(c)$	0.36 %
$Sm(yn)$	4.64 %

7. CONCLUSION

Thus, the conducted study suggest that in model and near-model problems solved by a direct method, a priory profile monotonicity information enhances the efficiency of profile

determination. Moreover, in some cases, it is impossible to obtain a solution without using this information. Firstly, it greatly decreases the probability of abends. Secondly, the use of monotonic functions ensures monotonicity of the resulting nozzle profile at all stages of computations. The best results are produced by *B*-splines for basis functions and by rational splines for interpolants.

Those problems including parameters characteristic of hypersonic wind tunnels, which could produce acceptable results, are essential in choosing an initial approximation and method for nozzle profile description.

Acknowledgements

The authors are thankful to A.N. Kraiko for useful discussion, N.E. Kuvshinov for computation by the relaxation method and McCormack scheme, A.F. Tsimbaluyk for computation by the relaxation method and Godunov scheme, and S.B. Khalimov for the program of computation up to the transonic part of a nozzle.

REFERENCES

[1] Kraiko, A.N. *Variational problems in gas dynamics*. Nauka: Moscow, 1979 [in Russian].

[2] *Theory of optimum aerodynamic shapes*. Edited by Miele, A. Academic press: New York, London, 1965.

[3] Kraiko, A.N.; Pudovikov, D.E.; Yakunina, G.E. *Theory of near-optimum aerodynamic shapes*. Yanus-K: Moscow, 2001 [in Russian].

[4] Butov, V.G.; Vasenin, I.M.; Shelukha A.I. Application of the methods of nonlinear programming to the solution of variational gas dynamics problems. *J. Appl. Math. Mech.* 1977, 41(1), 52–57.

[5] Dennis, J.E.; Schnabel, R. *Numerical methods for unconstrained optimization and nonlinear equations*. Prentice-Hall Inc.: New Jersey, 1983.

[6] Aulchenko, S.M.; Galkin, V.M.; Zvegintsev, V.I.; Shiplyuk, A.N. Design of a multimode axisymmetric nozzle for a hypersonic wind tunnel by methods of numerical optimization. *Abstracts of 14 International Conference on the Methods of Aerophysical Research*, Novosibirsk, 2008, 1, 221-222 [in Russian].

[7] Breev, V.V.; Gubarev, A.V.; Panchenko V.P. *Supersonic MHD - generators*. Energoatomizdat: Moscow, 1988 [in Russian].

[8] Butov, V.G.; Galkin, V.M.; Golovizin V.M., et al. *Numerical simulation of three-dimensional two-phase flows in supersonic MHD generators*. Preprint 5267/16, Kurchatov Institute of Atomic Energy: Moscow, 1990 [in Russian].

[9] Butov, V.G.; Galkin, V.M.; Khalimov, S.B. *Development of mathematical models and computation techniques for two-phase flows in space channel. Reg*. No. 01880031451, No. 02890062388, Report of the Institute of Applied Mathematics and Mechanics: Tomsk, 1989 [in Russian].

[10] Panchenko, V.P.; Dogadaev, R.V.; Koroleva L.A., et al. *Analysis of experiments on IM-1PE and recommendations for increasing the energy and lifetime characteristics of pulse MHD generators, 10/NIR – 3264-88*. Report of the division of the Kurchatov Institute of Atomic Energy: Москва, 1988 [in Russian].

[11] Galkin, V.M. Numerical investigation of two-phase flow in MHD generators on low temperature plasma. *Czech. J. Phys.*, 2002, D 52, 433–438.

[12] Afonin, G.I.; Butov, V.G. *Optimum nozzle configurations for two-phase flows*. Fluid Dyn., 1994, 29(2), 186-193.

[13] Ferri, A. *Elements of aerodynamics of supersonic flows*. The MacMillan Company: New York, 1949.

[14] Ryzhov O.S. *Transonic flows in Laval nozzles*. Vychisl. Tsentr Akad. Nauk SSSR: Moscow, 1965 [in Russian].

[15] Katskova, O.N. *Computation of equilibrium gas flows in supersonic nozzles*. Vychisl. Tsentr Akad. Nauk SSSR: Moscow, 1964 [in Russian].

[16] MacCormack, R.W. The effect of viscosity in hypervelocity impact cratering. *AIAA Paper* 69-354,Cincinati, Ohio, 1969.

[17] Galkin, V.M.; Volkov, Yu.S. Comparison of basis functions in the direct design problem for the supersonic part of a nozzle. *Sib. Zh. Ind. Mat.* 2004, 7(4), 48–58 [in Russian].

[18] Butov, V.G.; Khalimov, S.B. Calculation of nonpotential ideal gas flows in axisymmetric nozzles by the approximate factorization method. *U.S.S.R. Comput. Math. Math. Phys.*, 1987, 27(6), 170–174.

[19] Khalimov, S.B. *Numerical study of transonic ideal gas flows in complex-shaped nozzles*. Cand. sci. (phys. – math.) dissertation: Tomsk State Univ., Tomsk, 1988 [in Russian].

[20] Volkov, Yu.S.; Galkin, V.M. On the choice of approximations in direct problems of nozzle design. *Comput. Math. Math. Phys.*, 2007, 47(5), 882–894.

[21] Schumaker, L.L. *Spline functions: basic theory*. Wiley: New York, 1981.

[22] Aoki, M. *Introduction to optimization techniques*. The MacMillan Company: New York, 1976.

[23] De Boor, C. *A practical guide to splines*. Springer: New York, 1978.

[24] Miroshnichenko, V.L. Convex and monotone spline interpolation. *Proceedings of International Conference on Constructive Theory of Functions*, Varna, Publishing House of Bulgarian Academy of Sciences, 1984, 610-620.

[25] Späth, H. *Spline algorithms for curves and surfaces*. Utilitas Mathematica Publ. Inc.: Winnipeg, 1974.

[26] Byrkin, A.P.; Verkhovskii, V.P. *Supersonic axisymmetric contoured wind-tunnel nozzle*. Patent RF No. 1528116, 1993 [in Russian].

[27] Aulchenko, S.M.; Zamuraev, V.P. Design of a multi-regime nozzle by means of a direct method of numerical optimization. *Proceedings of 12 International Conference on the Methods of Aerophysical Research*, Novosibirsk, 2004, 1, 15-18 [in Russian].

[28] Galkin, V. M.; Zvegintsev, V. I. On the design of a multimode axisymmetric nozzle for hypersonic wind tunnel. *Proceedings of 4 All-Russia Scientific Conference on Fundamental and Applied Problems in Modern Mechanics*, Tomsk, Tomsk State Univ., 2004, 293–294 [in Russian].

[29] Korte, J. Aerodynamic design of axisymmetric hypersonic wind-tunnel nozzle using a least-squares/parabolized Navier-Stokes procedure. *J. of Spacecraft and Rockets*, 1992, 29(5), 685-691.